JOURNAL OF MATERIALS SCIENCE 31 (1996) 297–303

Characterization of microstructural damage during plastic strain of a particulate-reinforced metal matrix composite at elevated temperature

B. Y. ZONG*, B. DERBY
Department of Materials, University of Oxford, Parks Road, Oxford OX1 3PH, UK

The evolution of damage in a SiC-reinforced 2618 Al alloy during plastic strain has been investigated by elastic modulus reduction and direct observations of the microstructure at room temperature and temperatures up to 220 °C. Particle fracture increases as a function of strain at all temperatures but the total number of fractured particles at any given strain is lower at higher test temperatures. The dependence of fracture on particle size and aspect ratio was recorded. Normalized elastic modulus measurements decrease as a function of strain at the same rate for tests at 25, 110 and 220 °C with an anomalous set of measurements at 165 °C showing a reduced damage rate. There is no universal correlation between the number of damaged particles and reduced modulus with each test temperature showing a different relation. This indicates the different temperature dependence of void nucleation and subsequent growth. The results are used to interpret different models of load sharing between reinforcement and matrix during straining.

1. Introduction

Metal matrix composite materials (MMC) with combinations of low density, improved stiffness and strength, are sometimes seen as attractive alternatives to existing high-strength aluminium and titanium alloys. SiC particle-reinforced aluminium-alloy matrix composites are of interest because of their particular advantages of easy manufacturing and processing compared with other MMC systems. Some possible applications of SiC_p/Al-alloy MMCs require high-temperature mechanical performance, for example brake calipers, conrods and pistons in automotive applications, and airframe structures in supersonic aerospace applications. SiC_p/Al-2618 composite has potential as an elevated temperature MMC for use up to 250 °C because of its stable microstructure of intermetallic dispersoids. Spray deposition is particularly advantageous for 2618 alloys as it results in the refinement of the iron- and nickel-containing dispersoids. Also, this MMC has a lower potential cost than the higher strength aluminium–lithium alloys. Thus we have chosen SiC-reinforced Al-2618 as a suitable model material for the study of elevated temperature deformation in particulate-reinforced MMCs.

The poor ductility and fracture behaviour of MMCs are major concerns which limit their application. Another worry is the likely further deterioration of these properties after thermal and mechanical strain. The damage evolution which occurs during tensile testing of SiC_p/Al-2618 has been studied by Llorca *et al.* [1] by monitoring elastic modulus reduction with plastic strain at room temperature. These results were compared with predictions of stress distribution using finite element analysis. Here, the damage evolution of the SiC_p/Al-2618 composite will be investigated during plastic deformation at a range of temperatures up to 220 °C. These results will be compared with damage evolution measured in terms of the fraction of cracked SiC particles and also by measuring changes in the composite's elastic modulus. Void evolution in the matrix away from the reinforcement is also investigated after tensile testing.

Most previous investigations of SiC particle cracking in MMCs during plastic straining have been carried out on the outer surface of flat tensile test specimens [2, 3]. The free surface of the specimen will be in a state of plane stress during uniaxial tensile testing. However, the bulk of the material in the interior of the specimen will be in a condition closer to plane strain. Mummery and Derby [4] have shown that surface observations of particle damage tend to see a greater extent of damage than is seen from the interior of an MMC when a sectioned specimen is observed. In the present work we have taken all our measurements from specimen cross-sections.

The objective of this study was to assess the influence of temperature on the extent of damage as a function of plastic strain. The validity of elastic modulus measurement as a method of probing microstructural damage was investigated. This, in turn, was used to consider the models which have been used to predict

* *Present address*: Department of Materials, Northeastern University, Shenyang 110006, People's Republic of China.

load partition between matrix and reinforcement during straining.

2. Experimental procedure

The experimental materials were supplied by Alcan International Ltd, in the form of hot-extruded spray-formed billets. The composite had a nominal 15% volume fraction of SiC particles of approximate mean diameter of 10 μm in an Al-2618 (Al–2.5%Cu–1.5% Mg–1.1%Ni–1.1%Fe) matrix. A 530 °C solution treatment for 2 h was followed by an ice–water quench before the composite was machined into cylindrical tensile dumb-bell specimens of 5 mm diameter and 30 mm gauge length. The final specimens were aged at 200 °C for 20 h (peak-aged condition).

All tensile tests were carried out on a Mayes servo-electric testing machine model DM30 at a strain rate of $3.5 \times 10^{-5}\ s^{-1}$. Elastic moduli were measured throughout the tests by repeatedly unloading and reloading after different amounts of strain, using an extensometer and two type FLA-3-23 strain gauges on both sides of each specimen centre at room temperature, and type ZFLA-3 gauges at elevated temperatures. The modulus data were derived from the extensometer's measurements corrected by the first strain gauge's measurement because of the limited measurable strain range of the strain gauges. The plastic strain in the necked region after a tensile test was determined from the reduction in local area. Diameters of a specimen are measured along its gauge length from a marked edge with an interval of 0.25 mm before tensile testing using a laser micrometer which has a measured error of less than 0.6 μm. After the tensile test, the two fractured halves of the specimen are matched and stuck together with a tiny drop of glue, and then the local diameters of the specimen are measured again from the same marked edge. The local true strain of the specimen is determined by relation $\varepsilon_T = -2\ln(D/D_0)$ where D_0 and D are local diameters of the specimen before and after the tensile test, respectively.

After testing, the specimens were sectioned on a plane parallel to the loading direction and prepared for metallographic observation in the conventional manner. The microstructure of the composite specimens after tensile testing was examined on polished longitudinal sections by means of a Quantimet 900 optical microscope which is equipped with a computer-controlled image analysis system to determine the local volume fraction, number and geometric features of selected broken SiC particles. The broken SiC particles were distinguished from all SiC particles on screen manually.

3. Results and discussion

3.1. Microstructural damage and elastic modulus reduction

It is impractical to study damage evolution of the composite during deformation by measuring fractions of broken SiC particles on sectioned specimens after various tensile strains, for two reasons. Firstly, it is difficult to compare data which come from different specimens and different tests. Secondly, local true strains are not constant along the gauge length of a specimen after significant tensile extension. However, if local true strains can be measured accurately, a set of damage evolution data can be obtained from a single specimen by measuring local fractions of broken SiC particles. The composite under study has the advantage of an early and slowly changing gradient of necking which offers areas on tested specimens with a range of locally distinguishable strains. Fig. 1 shows an example of the local diameter of a specimen before and after a tensile test measured by laser micrometer. The local true strains of the specimen after the test can be determined assuming that deformation is distributed evenly along the specimen's transverse section perpendicular to the tension axis. We believe this assumption to be valid because the specimen's transverse sections are still very circular after tensile testing with a diameter variation less than 1%.

After measuring their local diameters, fractured specimens are sectioned in a longitudinal direction along the tension axis by spark erosion, to avoid extra mechanical damage, and then polished. One of microstructures obtained is shown in Fig. 2 taken just

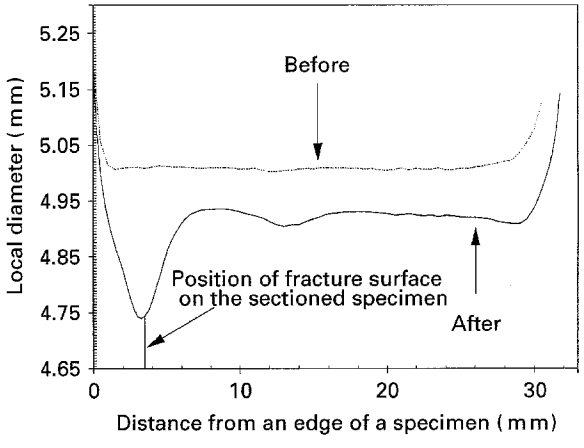

Figure 1 Local diameter, measured by laser micrometer, as a function of distance along a specimen before and after the tensile test at 165 °C.

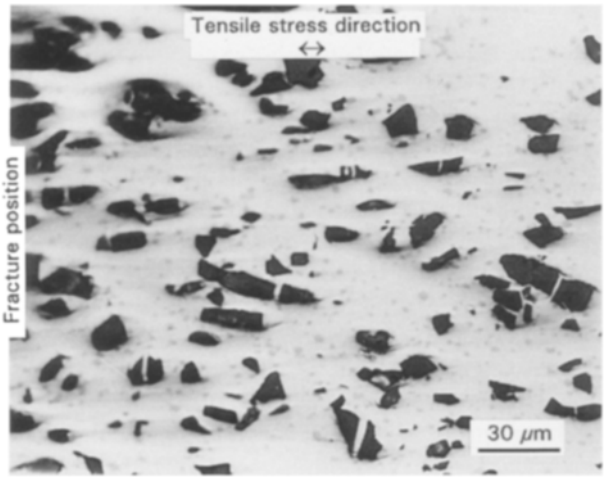

Figure 2 Longitudinal section of a typical fractured tensile specimen used to measure the local fraction of broken SiC particles beneath the fracture surface.

beneath the fracture surface. Most of the cracks on the broken SiC particles appear white, not black as might be expected. This could be the result of the cracks being very narrow and aluminium smearing during polishing and filling them in. Fig. 3 is a plot of the measured local fractions of broken SiC particles as a function of position. There is significant scatter in the fraction of broken particles measured across the specimen at the same distance from the fracture surface which are nominally at the same state of strain. However, any single datum which is used to show the relationship between SiC cracking and plastic strain is obtained from at least 14 measurements taken randomly across a specimen at the same local strain.

The test results showing damage evolution as the fraction of SiC particles cracked during tensile deformation, for a range of temperatures up to 220 °C, are given in Fig. 4. At room temperature, up to 20% of the SiC particles can be broken after a plastic strain of less than 0.1 before the specimen fails. When tested at elevated temperature, many fewer SiC particles are broken for any given plastic strain. The rate of composite damage evolution as a function of strain is slowest at high temperatures, however, there is an increase in damage rate to greater than the room temperature value at the intermediate temperature of 110 °C. This suggests that the damage and recovery mechanisms show different temperature activation, i.e. at high temperature the particle stress is reduced by some time-dependent process.

Damage evolution can also be evaluated by measuring elastic modulus reduction during tensile deformation. Results using this method are shown in Fig. 5a. The elastic modulus of the composite at zero plastic strain decreases gradually as temperature increases from 25 °C to 165 °C and this is consistent with the reduction in matrix modulus with temperature. Fig. 5b shows the modulus reduction data as a damage parameter normalized by the modulus at zero strain. The modulus reduction rate is nearly the same at both 25 and 110 °C. The data measured at room temperature, 110 and 220 °C all lie on the same line. However, the modulus reduction data at an intermediate temperature of 165 °C are anomalous. A similar intermediate temperature anomaly was seen with the cracked particle fraction but at the lower temperature of 110 °C.

In order to compare the two damage parameters, we have plotted the normalized elastic modulus reduction as a function of the fraction of broken particles measured at a given strain. Fig. 6 shows that the elastic modulus reduction of the composite is consistent with an increasing fraction of broken SiC

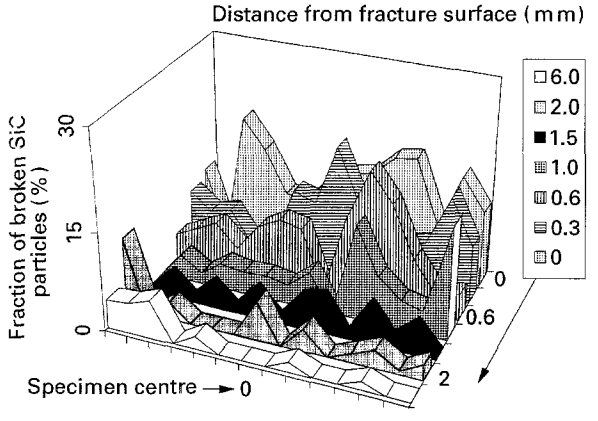

Figure 3 Local fractions of broken SiC particles measured from a longitudinal section of a fractured specimen after tensile test at 165 °C.

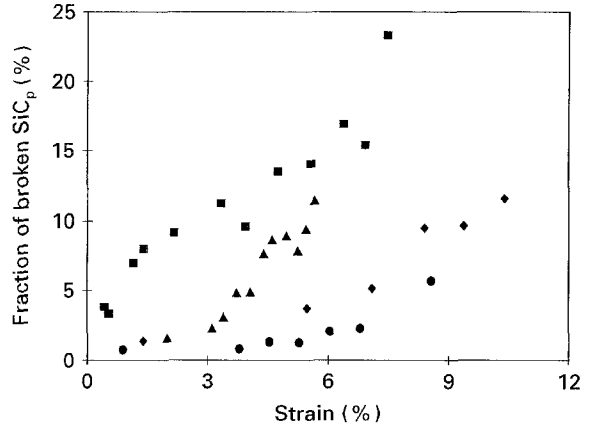

Figure 4 The fraction of broken SiC particles as a function of tensile strain over a range of temperatura typical fractured tensile specimen used to measure the local fraction of broken SiC particles beneath the fracture surface.

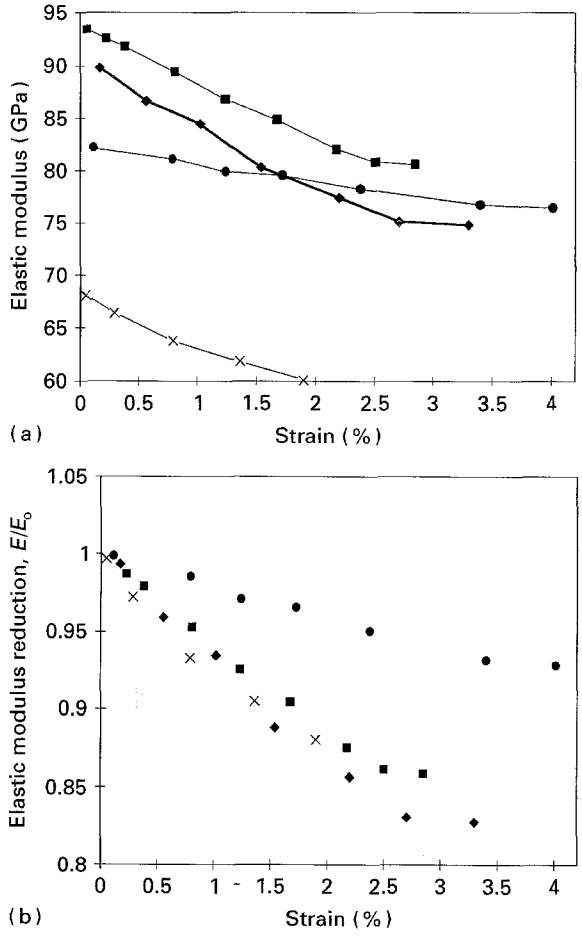

Figure 5 (a) Elastic modulus reduction of the composite as a function of tensile strain over a range of temperatures up to 220 °C, (b) normalized by the modulus at zero strain. (■) 25°C, (◆) 110 °C, (●) 165 °C, (×) 220 °C.

particles during strain at all test temperatures. Thus, elastic modulus reduction can be used to represent microstructural damage of the composite in a qualitative manner. However, the considerable divergence seen in the data of Fig. 6 shows that there is no simple relationship between the number of broken particles and the reduction in elastic modulus which can be applied at all test temperatures. Indeed if such a relation were valid we would expect all four experimental results to lie on a common master curve. The deviation occurs when the fraction of broken particles is about 2% which, from Fig. 4, is at strains well below that at which strain localization is likely. Hence the lack of a common relation between modulus and microstructure suggests that another factor, the total volume fraction of voids is the controlling parameter. Thus both the void nucleation rate and the void growth rate are important in determining the reduction in modulus. The data in Fig. 6 only account for nucleation and not growth, which is expected to become more rapid with increasing test temperature.

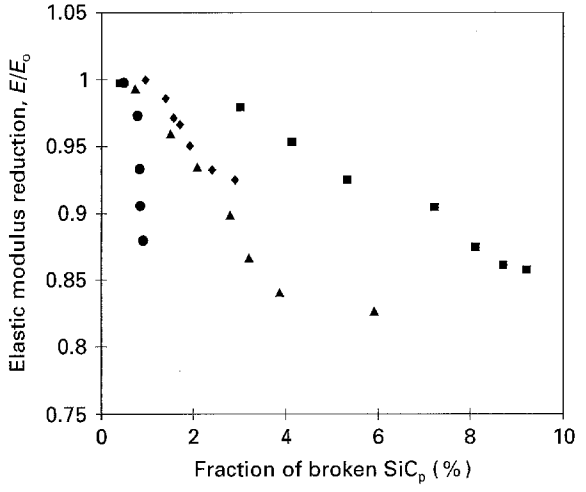

Figure 6 The elastic modulus reduction plotted against the fraction of broken SiC particles in the corresponding specimens over a range of temperatures up to 220 °C: (■) 25 °C, (▲) 110 °C, (◆) 165 °C, (●) 220 °C.

3.2. Characterization of broken SiC particles and voids

Microstructural observation of sectioned specimens after tensile fracture in Fig. 7 shows that void coalescence only occurs at some SiC particle clusters and individual SiC cracks do not open significantly with further strain. In Fig. 7c, some very small voids can be seen near $FeNiAl_9$ precipitates, as well as near SiC particles in this SEM backscattered electron image. The voids in the matrix cannot be identified by optical microscopy because of their small size and aluminium smearing during specimen polishing. Microstructural observation of sectioned specimens after tensile fracture also reveals some typical features of the broken SiC particles. Firstly, after small strains, the SiC particles with large aspect ratios along the tension stress direction are easily broken regardless of particle size as seen in Fig. 8a. Fig. 8b shows that amongst the blocky SiC particles, large ones tend to be broken at smaller plastic strains. Some cracks occur at thin tails or sharp corners of the SiC particles (Fig. 8c), and in Fig. 8d some broken SiC particles show a further shear displacement after being cracked. At large strains, some shattered SiC particles and some broken SiC particles with multiple cracks appear (Fig. 9a). Moreover, the average size of broken SiC particles can be smaller

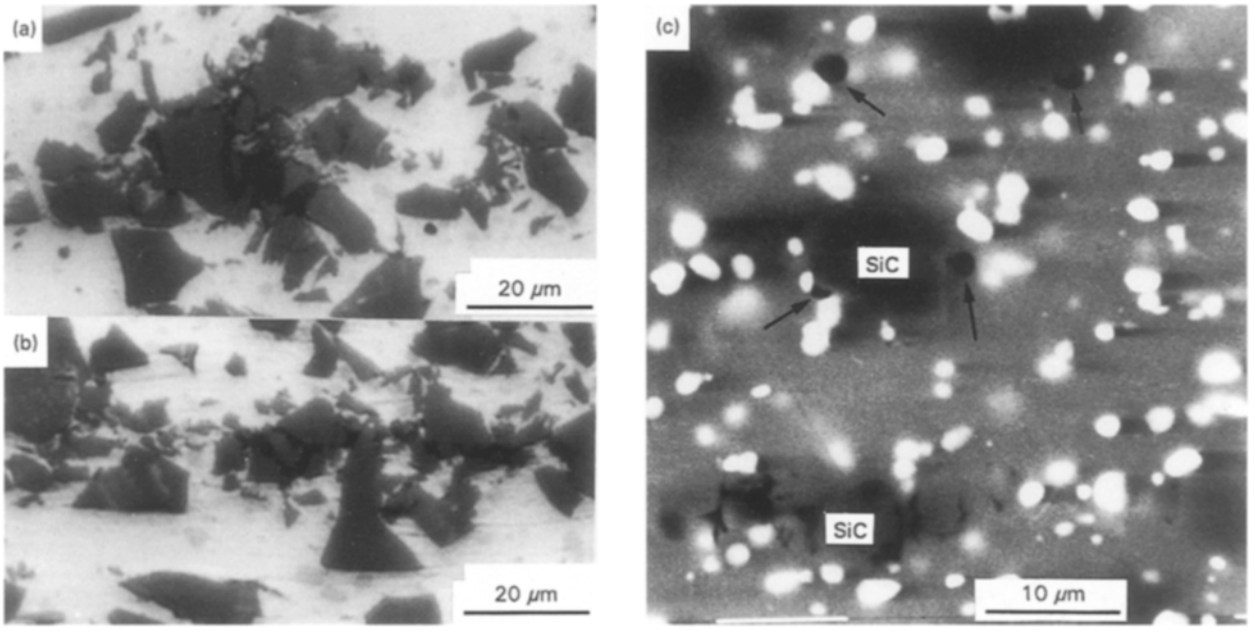

Figure 7 (a, b) Optical micrographs showing void coalescence close to clustered SiC particles in the composite after tensile strain, (c) SEM backscattered electron image showing void nucleation by decohesion at intermetallic particles (bright features) and by particle fracture at an SiC particle (bottom of micrograph).

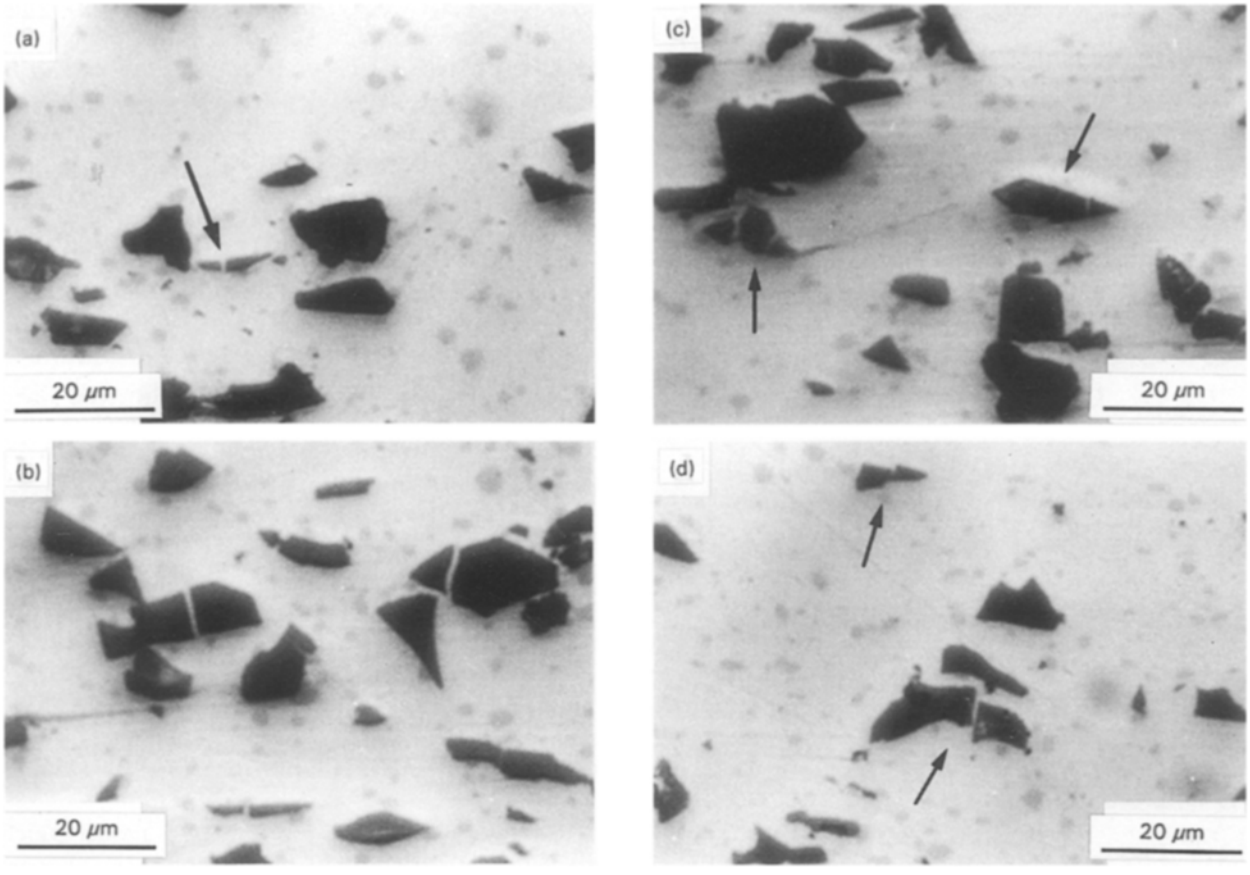

Figure 8 Typical features of broken SiC particles after tensile tests to small strains. (a) Even very small particles with large apsect ratios along the tensile stress direction break at an early stage of deformation. (b) Large equiaxed block-shaped particles are broken first. (c) Thin tails or corners of the particles are easily broken off. (d) Some broken particles show a further shear displacement.

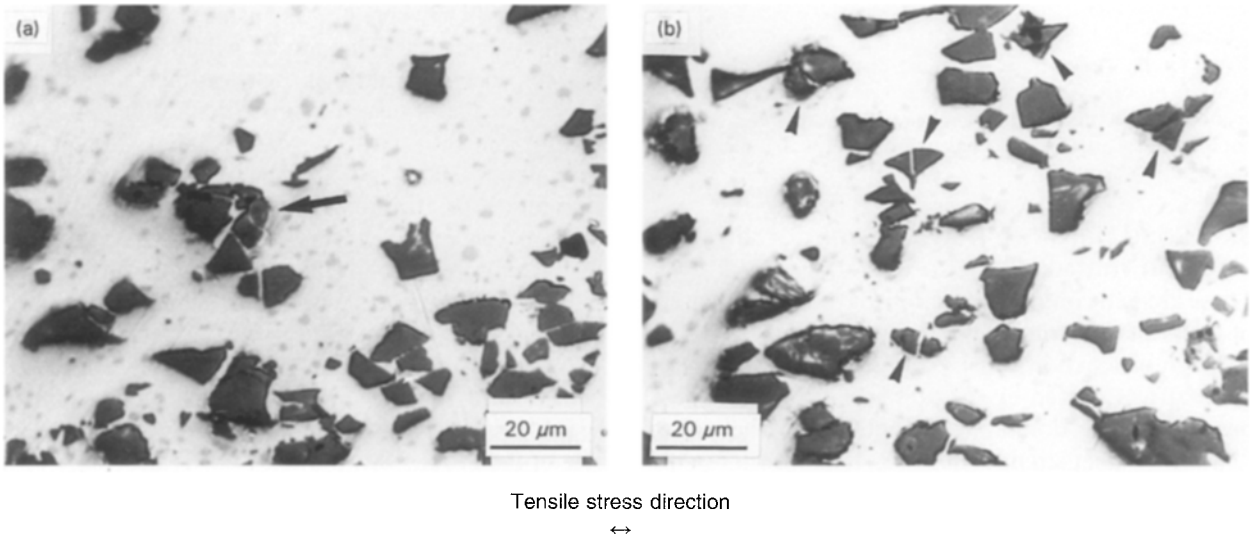

Figure 9 Typical features of broken SiC particles during tensile tests to large strains. (a) Shattered SiC particles (arrowed). (b) Some small particles are broken (arrowed) even when they have large unbroken neighbours.

than the surrounding unbroken SiC particles in Fig. 9b.

Fig. 10 shows that both the average aspect ratio (D_{max}/D_{min}) and the average aspect ratio resolved along the tensile stress direction (D_x/D_y) of the broken SiC particles decrease with increasing strain after tensile testing at 165 °C. D_{max} and D_{min} are the maximum and minimum diameters of a broken SiC particle measured along four diameters in different directions which are along the tensile stress direction (x-axis), 45° direction from the x-axis, 90° direction (y-axis) and at 135° from the x-axis. From Fig. 10, it can be seen that the plot of aspect ratio projected along the tensile stress direction (D_x/D_y) shows less scatter than that of D_{max}/D_{min}. The average maximum diameter (D_{max}) and the average diameter calculated from the measured particle area (D_{area}) of broken SiC particles are presented in Fig. 11 against the deformed strain after tensile tested at 165 °C, where $D_{area} = (4A/\pi)^{1/2}$ and A is the measured area of a broken SiC particle on the specimen sections. From Fig. 11, it is clear that the D_{area} curve also shows much less scatter than the D_{max} curve.

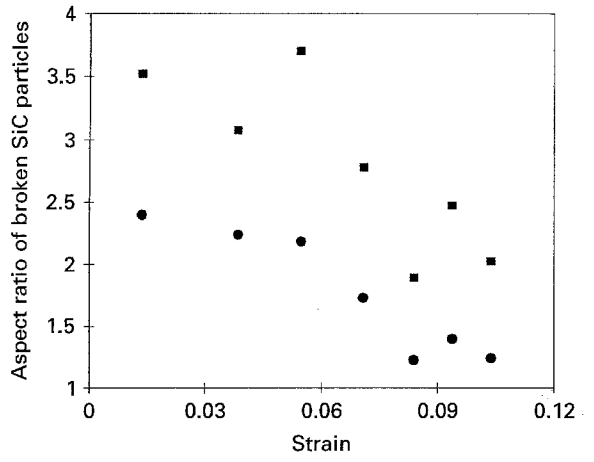

Figure 10 Aspect ratios of broken SiC particles (■, D_{max}/D_{min}) and aspect ratios along the tensile stress direction (●, D_x/D_y) after testing at 165 °C. X is tensile stress direction axis and Y is the vertical axis.

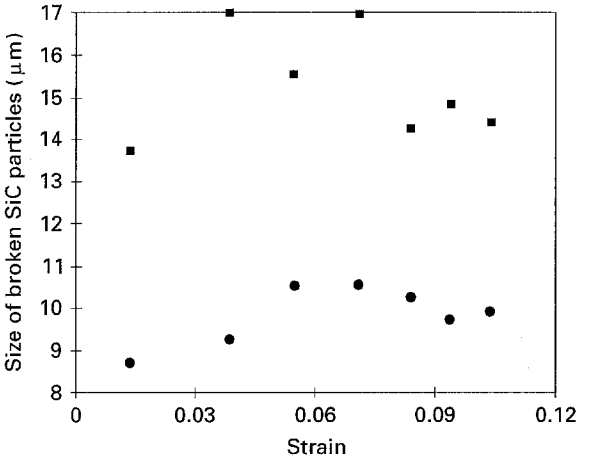

Figure 11 (■) The average maximum diameter, D_{max}, measured from the broken particles and the equivalent mean diameter calculated from (●) the measured broken particle areas, D_{area}, assuming a spherical particle, as a function of local strain after tensile testing at 165 °C.

3.3. Load partition between reinforcement and matrix

These are two controlling factors for the strengthening of metal matrix composites. In low-strength matrices the high dislocation density and the fine grain size of the matrices caused by the presence of reinforcement particles is the dominant strengthening mechanism [5]. With higher strength matrices, load transfer to the particles is more important because the microstructural strengthening mechanisms are smaller than those provided by precipitates or dispersoids. Fig. 4 shows that some SiC particles are cracked at a very early stage of deformation, especially at low temperatures, which is strong evidence that load transfer to the SiC particles is an important factor in strengthening the Al-2618 matrix MMC. The SiC particles can be broken by uniaxial tension only when the stress in the particles exceeds their strength. Assuming all the particles to have a diameter of 10 μm and a fracture toughness of 4 MPams$^{1/2}$, if the maximum crack size in a particle is taken as half the particle diameter, a simple application of the fracture mechanics suggests a minimum failure stress of 1 GPa. If the stress in all the SiC particles in the composite just before composite failure is assumed to be around their mean fracture strength, which we take to be approximately 2 GPa, from Fig. 4 about 10% of all SiC particles just beneath the fracture surface were broken before the specimen was fractured by tension at 165 °C, the upper bound for the load sustained by the SiC particles could be as high as 49% of the total load at 165 °C according to the rule of mixtures.

The mean aspect ratios of the broken SiC particles and their aspect ratios along the tensile stress direction in Fig. 10 are much larger than those measured for all SiC particles in the composite which were 1.79 and 1.06, respectively [6]. This fact indicates that a shear-lag mechanism plays a role in the load transfer from the matrix to SiC particles in the composite during straining. However, workers using the shear-lag model have concluded that the stress in the SiC particles in the composite can only reach the level of the fracture strength when their aspect ratio along the maximum tensile stress direction is larger than 4 [7]. The observed aspect ratio of the broken SiC particles along this direction in Fig. 10 is, however, less than 2.5 even at the lowest strain. This means that load transfer to the SiC particles cannot be explained by a simple shear lag.

Brown and Stobbs [8] proposed a model which predicts that the stress within an undeformable particle in an infinite plastic matrix is built up during plastic strain of the matrix by the accumulation of dislocations around it, regardless of its aspect ratio. This model predicts the particle stress, σ_p, as a function of far-field strain, ε, and particle diameter, d, with $\sigma_p = C(\varepsilon/d)^{1/2}$ (where C is a constant related to matrix elastic properties). This model would predict an increasing size of broken particles with strain and can only meet the observed microstructural behaviour of the broken SiC particles when plastic strain is less than about 0.06 (Fig. 11). Eshelby's equivalent inclusion model [9, 10] predicts no relation between strain and broken particle size with $\sigma_p = X\varepsilon$ (where X is a constant related to the elastic properties of the particle and the matrix, and also the particle volume fraction). This model appears to be better than the Brown and Stobbs model considering the observed behaviour of the broken SiC particles in Fig. 11 when plastic strains are larger than 0.06. However, the mean size of the broken SiC particles slowly decreases with increasing strain once the strain is larger than 0.06. This suggests that, in addition to the Brown and Stobbs and the Eshelby models, a further consideration of the effect of the SiC particle's strength as a function of particle size is needed to meet the microstructural damage characteristics of the SiC particles in detail. This could be achieved either by using arguments based around Weibull statistics or else by invoking a maximum defect-size criterion related to the particle-size distribution.

4. Conclusion

The local true strain along a specimen's gauge length has been determined by measuring the local diameters

of the specimen before and after tensile testing. Local fractions of broken SiC particles and their features were measured on the specimen's longitudinal section by means of image analysis and correlated with strain. Damage evolution within the composite was also investigated in terms of elastic modulus reduction during tensile testing at a range of temperatures up to 220 °C.

The fraction and nature of broken reinforcements as a function of strain can be evaluated within the necked region of a single specimen using this method.

Damage evolution of the composite in terms of its elastic modulus reduction is consistent with microstructural observations of SiC particle cracking.

Although SEM observations show some small voids near Al_9NiFe precipitates in the matrix at an early stage of strain, voids are always enlarged, and coalesced around clustered SiC particles near the fracture surface at large local strain.

Characterization of the broken SiC particles after tensile straining shows that SiC particle load sharing is an important strengthening effect in the composite. However, neither shear lag, Eshelby's equivalent inclusion nor Brown and Stobbs [8, 9] dislocation models for the loading of a particle in a plastic matrix, can adequately explain the observed features of the microstructural damage during strain.

Acknowledgements

The authors thank Alcan International Ltd for supplying the materials and EPSRC for financial support under grant GR/H33817. B. Y. Zong thanks the Chinese Education Commission and the British Council for a Cooperation Scholarship. Dr. C. Lawrence is thanked for assistance with the laser apparatus.

References

1. J. LLORCA, A. MARTIN, J. RUIZ and M. ELICES, *Metall. Trans.* **24A** (1993) 1575.
2. D. J. LLOYD, *Acta Metall. Mater.* **39** (1991) 59.
3. P. M. SINGH and J. J. LEWANDOWSKI, *Metall. Trans.* **24A** (1993) 2531.
4. P. M. MUMMERY and B. DERBY, *J. Mater. Sci.* **29** (1994) 5615.
5. S. W. MILLER and F. J. HUMPHREYS, *Scripta Metall. Mater.* **25** (1991) 33.
6. B. Y. ZONG and B. DERBY, *J. Phys. IV C7* **3** (1993) 1861.
7. V. C. NARDONE and K. M. PREWO, *Scripta Metall.* **20**, (1986) 43.
8. L. M. BROWN, and W. M. STOBBS, *Philos. Mag.* **34** (1976) 351.
9. J. D. ESHELBY, *Proc. R. Soc. Lond.* **241** (1957) 376.
10. T. MOCHIDA, M. TAYA and D.J. LLOYD, *JIM* **32** (1991) 931.

Received 12 May
and accepted 22 June 1995